Journal of Intelligent & Fuzzy Systems xx (20xx) x–xx
DOI:10.3233/JIFS-212189
IOS Press

A Hybrid deep learning model for effective segmentation and classification of lung nodules from CT images

Malathi Murugesan[a,*], Kalaiselvi Kaliannan[b], Shankarlal Balraj[c], Kokila Singaram[d], Thenmalar Kaliannan[e] and Johny Renoald Albert[f]
[a]*Department of ECE, Vivekanandha College of Engineering for Women (Autonomous), Namakkal, Tamilnadu, India*
[b]*Department of Networking and Communications, SRM Institute of Science and Technology, Kattankulathur, Kanchipuram Dt, Tamil Nadu*
[c]*Department of ECE, Perunthalaivar Kamarajar Institute of Engineering and Technology, Karaikal, Puducherry, India*
[d]*Department of ECE, Vivekanandha College of Engineering for Women (Autonomous), Tiruchengode, Namakkal*
[e]*Department of EEE, Vivekanandha College of Engineering for Women (Autonomous), Elayampalayam, Namakkal*
[f]*Department of EEE, Vivekanandha College of Engineering for Women (Autonomous), Elayampalayam, Namakkal*

CORRECTED PROOF

Abstract. Deep learning algorithms will be used to detect lung nodule anomalies at an earlier stage. The primary goal of this effort is to properly identify lung cancer, which is critical in preserving a person's life. Lung cancer has been a source of concern for people all around the world for decades. Several researchers presented numerous issues and solutions for various stages of a computer-aided system for diagnosing lung cancer in its early stages, as well as information about lung cancer. Computer vision is one of the field of artificial intelligence this is a better way to detect and prevent the lung cancer. This study focuses on the stages involved in detecting lung tumor regions, namely pre-processing, segmentation, and classification models. An adaptive median filter is used in pre-processing to identify the noise. The work's originality seeks to create a simple yet effective model for the rapid identification and U-net architecture based segmentation of lung nodules. This approach focuses on the identification and segmentation of lung cancer by detecting picture normalcy and abnormalities.

Keywords: Lung cancer, pre-processing, support vector machine, deep learning, U-Net, classification accuracy

1. Introduction

Cancer is well-known for its uncontrolled widening and alteration of cells in the human. The human body is made up of small, blocked pieces called cells. Normal cells transmit when the body requires them and perish when they are not required. Cancer is made up of non-uniform cells that grow even when the body does not need them. The abnormal cells multiply to form a bulge or lump known as a tumor. If cancer cells remain in the body for an extended period, they can colonize (invade) nearby tissues. They even spread to other parts of the body (metastasis). Lung cancer is the leading cause of

*Corresponding author. Malathi Murugesan, M.E., Ph.D, Assistant Professor, ECE, Vivekanandha College of Engineering for Women, Tiruchengode, Namakkal, 635207 Tamilnadu, India. E-mail: m_malathi123@rediffmail.com.

ISSN 1064-1246/$35.00 © 2021 – IOS Press. All rights reserved.

cancer-related death globally. Non-Small Cell Lung Cancer (NSCLC) victims account for around 80% of every lung cancer case, with the majority having a locally metastatic or advanced illness. Many individuals are identified with lung cancer in its advanced stages and have a systematic or local modern illness (phase 3 or 4) with a 5-year survival rate of 5%. Victims of lung tumors die more than 50% of cases during the early time after diagnosis [1]. As a result, there is a greater demand for innovative treatment and diagnostic choices that rely on particular biomarkers, ideally identifiable in cancer surrogate cases acquired by the non-invasive strategy. Because of the non-invasive and simple access for detectable genetic material in the serum and plasma using the sensitive molecular method, the detection of intercellular DNA flow in the blood and called cf DNA (cell-free DNA) has a significant impact on lung cancer victims' molecular diagnostics.

Lung cancer begins in the cells that form the lungs. Many other kinds of tumors, like kidney or breast cancer, metastasize (feed) on the lungs. When this occurs, the tumor is not referred to be a lung tumor. This is determined by the location of the early malignancy. If a breast tumor spreads to the lungs, it is considered a metastatic breast tumor rather than a lung tumor. The lungs are sponge-like organs in the chest. The lung's function in the human body is to transport oxygen into the body and remove carbon dioxide. When people inhale, oxygen enters the lungs via the windpipe. Then the windpipe divides into tubes known as bronchi, which invades within the lungs. These are divided into tiny branches called bronchioles. At the end of the bronchioles are little balloons called alveoli. Through the process of breathing, the alveoli carry oxygen into a person's blood. Furthermore, by exhaling, carbon dioxide is taken from the blood and expelled from the body [2]. In humans, the right lung is isolated to three segments (lobes), and the left lung is isolated to two segments. These two types spread and nurture in different ways. They are also frequently treated differently. Non-small cell lung cancer accounts for around 84–91 percent of all lung tumors in NSCLC.

They are divided into three categories based on the type of lung cell in which the tumor begins and by examining the cells under a microscope. However, there will be very little difference between them. Adenocarcinoma, squamous, and big cell carcinoma are the three kinds; adenocarcinoma is a sort of mutual NSCLC. People who do not smoke are more likely to develop adenocarcinoma type lung cancer. However, they are more commonly found in former smokers or smokers. This form of lung cancer is more likely to develop on the outer side of the lungs and to produce moderately than other types of lung cancer. The next kind of NSCLC epidermoid carcinoma (squamous cell carcinoma) frequently develops in former smokers or smokers. These tumors first appear in the middle area of the lung, near the bronchi (airways). The least common form of NSCLC is large cell carcinoma. These have a propensity to rapidly feast and progress to other areas. SCLC (Small cell lung cancer), also called oat cell cancer, has afflicted roughly 11–16 percent of individuals. It feeds and grows more quickly than non-small cancers [3]. During the initial stage, it frequently feasts on various body parts.

The lymph nodes in the center of the chest are the most prevalent location where lung cancer spreads. These lymph nodes are referred to as mediastinal nodes. The aggressiveness of lung cancer has also extended to the lymph nodes in the lower neck. Lung cancer has recently expanded (metastasized) to other areas of the body, such as the brain, liver, or bones. A feature number may increase a person's risk of lung cancer. Definite risk factors can be reduced, for example, by quitting smoking. Some characteristics, such as a person's familial history, are uncontrollable. Smoking, exposure to a smoker, radon gas, asbestos, and toxins are all risk factors for lung cancer. The number of cigarettes smoked each day enhances the risk of evolving lung cancer. Stopping at any time significantly reduces the chance of evolving lung cancer. Even if they are not a smoker, being exposed to someone who smokes increases their chances of developing lung cancer. Office exposure to asbestos and elements such as chromium, nickel, and arsenic has been linked to cancer. People who have a mother, a brother, a father, a kid, or a sister who has lung cancer possess a more risk. Figure 1 depicts noncancerous and malignant pictures.

Because symptoms appear only in late stages, detecting a tumor in the initial stages is difficult, resulting in lung cancer has the highest death rate of any kind of cancer. Even skillful radiologists possess trouble discerning the true pattern of dividing blood arteries in the field of the lungs or identifying tiny nodules which denote lung cancer. While radiologists determine the seriousness of abnormal findings, substantial and even intra-observer variance happens [4]. The clinical significance of chest radiographs, along with their complexity, describes the desire to evolve computer designs to aid radiologists

CORRECTED PROOF

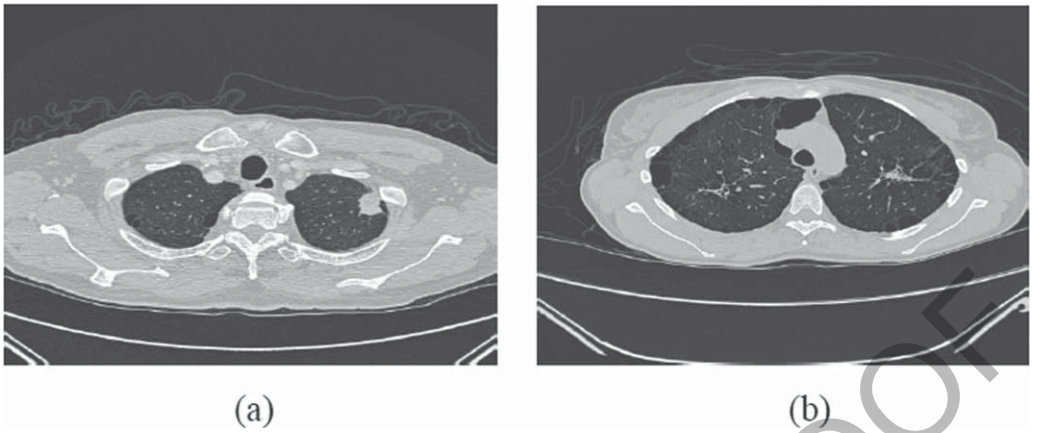


Fig. 1. a) Non-Cancerous; b) Cancerous.

in grading chest figures. These are challenges that are beyond the scope of current training approaches and clinical skill levels and expertise. These difficulties also include the rate of missed small pulmonary nodules, detecting changes in prior intestinal illnesses, and determining the minimal interstitial disease in the lung. Though traditional classifiers are frequently employed for image classification, the propagation design of ANN is a preferable alternative for TB and cancer image classification. The supervised trained architecture produces results faster than the classic classifier, however, to produce structured results, the support vector machine maps figures onto the hyperplane, dividing them into two linear distinct phases that allow classification.

As a result, the problem to address for first lung cancer detection is related to lowering the number of FP classifications if maintaining a prime degree of TP (true-positive) diagnosis, which is sensitivity. Various approaches were presented to decrease the quantity of FPs if nourishing sensitivity. Nearly 40% of lung lumps are malign, or dangerous; the remainder is generally connected with infections. Since malignancy is determined by numerous criteria, including nodule form, the presence of calcification, patient age, and doubling time, further examinations are required after the first nodule is detected. Segmentation in computer vision relates to the procedure of dividing a digital figure into pixel sets or several areas. Every pixel in the sector has the same calculated attribute or characteristic, such as texture, color, or intensity [5]. Adjacent sectors are symbolically distinct in terms of comparable features. The importance of the first diagnosis in terms of prognosis and therapeutic planning cannot be overstated. Thus, nodules are the well-known signs of lung cancer, and nodule identification in CT scan figures is the primary diagnostic concern. Conventional prediction radiography is inexpensive, straightforward, and mostly utilized for clinical testing.

Lesions are small and do not contrast well with anatomical form. This describes why specialists are typically credited with little sensitivity in the identification of a nodule, with ratings ranging from 60% to 70%. In many countries, lung cancer is the prime cause of tumor mortality in men. Lung cancer is classified into four stages, I through IV, with increasing severity. If a tumor is found in phase I and is no wider than 30 mm in width, there is a 67 percent chance of survival and just a 1% chance of progression to phase IV. As a result, it is determined that early identification and therapy at stage one have a more chance of survival. A comprehensive examination of the disadvantages impacting traditional chest radiography is provided. A significant long-term study, however, was done in the 1980 s utilizing vast clinical data recorded till 90 percent of nodules were properly obtained retrospectively. Furthermore, the observation sensitivity has been enhanced by more than 80% of the people in the event of the double radiograph evaluation through two radiologists. Moreover, sensitivity is awaited to improve with the usage of digital radiography technologies that are characterized by a greater dynamic level and a higher contrast intention than traditional film radiography. Considering this, the accessibility of effective and efficient CAD models is very desirable, while such approaches are often designed to give the physician the next opinion. The

CORRECTED PROOF

purpose of this study is to make a comparison of the performance of CNN + SVM classifiers in producing an online cancer database. Different calculation parameters, such as sensitivity, accuracy, specificity, false positive and negative, true positive and negative, are utilized to analyze both classifiers. As a result, early detection of lung cancer contributes to a lower death rate. The paper consists of related works in section 2 followed by the method in section 3. Section 4 presents the findings of the experiments, followed by Section 5's conclusion.

2. Related works

The current approach in the literature offered a new automatic diagnosis classification method to CT (Computed Tomography) lungs figure. A CT scan of the lung figure was analyzed using ODNN and LDA [6]. Deep attributes are removed from the CT lung image, and feature dimensionality is later decreased by utilizing LDR for classifying lung nodules as benign or malignant. Thus the ODNN was looking for CT figures, which were then optimized by utilizing MGSA to find lung cancer analysis.

Another method compares CNN design implemented by using various plans in CT estimate of EGFR mutation condition in victim with lung adenocarcinoma [7]. 1,010 successive lung adenocarcinoma victims with accepted EGFR mutation conditions were randomly split into testing sets ($m = 200$) and training sets ($m = 810$). The CNN design build-up depends on ResNet-101 construction but it is achieved by applying various plans: (2D/3D) dimension filters, slicing designs, input sizes (fusion and small/large/middle), and training access. The CNN designs performance compared utilizing AUC. Thus the fusion access yielded always good conductance than alternative input amounts, though the development generally did not attain analytical significance. The multi-view slicing automatically higher to transverse design while adjusting a pre-experienced 2D CNN but not for CNN trained against scratch. Whereas, the 3D CNN significantly advances than 2D transverse plane design but alone marginally advances than multi-view slicing design during trained against scratch.

An effective method aims for community and classifies malignant improvement in the lung, by the CNN method [8]. The author presented a model which utilized CNN for procedure tumors that were classified as amiable or dangerous in lung illness screening understanding tomography filters. The CNN's have a remarkable appearance, like taking into detail spatial invariance at various part abstraction. As a more mechanized methodology, the CNN model utilized picture data as input data and was straightforwardly restricted as yield.

A novel model based on deep learning with several strategies was recommended for the precise detection of malignant lumps [9]. Detections of nodule executed through rapid R-CNN on accurately learned appearance from U-Net and CMixNet related encoder-decoder construction. Analysis of nodules executed through a GBM on studied attributes from the 3D CMixNet designed structure. Deep learning design for lumps' classification and detection, connected with clinical aspects, aids in the lowering of false-positive and misdiagnosis outcomes in first-step lung cancer identification.

Another method described a data-driven framework named DB-ResNet. In this approach, two novel schemes were combined for developing the generalization capacity of the framework: 1) the present system simultaneously arrests multi-scale and multi-view appearances of various lumps in CT figures; 2) Next combine the appearances of the CNN and the intensity. And a pooling design was introduced, called CIP, to remove the intensity appearance of the middle voxel block, and utilize CNN for obtaining the convolutional appearances of the middle voxel block [10]. In inclusion, by constructing a weighted measuring plan that depends on nodules boundary for selecting these voxels applying the weighting amount, the model accuracy was enhanced. The proposed system largely calculated on the LIDC dataset involves 986 lumps.

An effective method [11] in literature concentrates on a coarse-to-fine segmentation of the lung nodule system by connecting the image improvement and the Dual-branch neural structure. Earlier, the author pre-processes the image to increase the nodules discrimination and approximately locate lesion region so ignore noises from the background and target on studying the appearances around the edges. Next, Dual-branch associates depend on U-Net (DB U-Net) successfully analyzed data from the two 2D slices and the communication in the middle neighbouring slices, to better precise and logical segmentation. In inclusion, a dataset is constructed that was mainly confident of the non-solitary nodules.

An effective method explains the two-stage CNN (TS-CNN) construction for lung nodule recognition [12]. The CNN construction in the initial stage

CORRECTED PROOF

depends on a developed U-Net segmentation structure for build a basic recognition of the lung nodules. Simultaneously, to obtaining a more recall amount without submitting extra false positive nodules, the author introduces a new sampling approach and utilizes disconnected hard mining concepts to predict and train according to recommended cascaded prediction system. The CNN construction in the second step depends on the present dual pooling design that was constructed into 3D CNN allocation networks for false-positive reduction. As network training needs a significant training data amount, the author adopted a data augmentation system that depends on the irregular mask. Moreover, the author developed the generalization capacity of false-positive reduction figures by measures of ensemble study. The present system analytically verified the LUNA dataset.

A novel method for training deep neural networks used diameter data to every nodule and also based on probability based computation have been effectively proposed in the literature [13–15]. The design was validated with the LUNA16 dataset and competitive outcomes related to earlier state-of-the- art designs in different calculation metrics were obtained.

Another method presents a framework for precisely observe lung cancer through classifying in the middle of malignant and benign lumps. The model was tested utilizing the public subset available at the database LIDC-IDRI. Multiple models including noise removing and filtering were used for pre-processing [16]. Then, semantic segmentation and the OTSU were utilized for identifying the unhealthy lung nodules accurately.

An effective method based on MV-SIR CNN design to 3D segmentation of lung nodule applying the LIDC-IDRI dataset of the chest CT pictures. Lung nodule hexahedrons were planned from the pattern CT pictures. Moreover, from sagittal perspectives, coronal, axial, and multi-view bits were achieved with aimlessly preferred voxels in lung nodule hexahedrons as places. Our design [17] subsists of six subfigures, that enable studying of 3D nodules of lung divide into three consider of appearances: each sub-figure excerpt voxel and shape heterogeneity appearances. And convert 3D lung lumps segmentation to voxel analysis by loading multi-view repair into the design and resolve whether voxel points fit the nodule. Then the architecture of the secondary input enduring sub-model constituted an enduring block pursued by a secondary input component. Then combined the six sub-figures to arranging whether voxel points fit lumps and recreate the segmentation picture.

Another method employed the strong object identification neural system "Mask R-CNN" to segmentation of lung nodule that produces contour data [18]. Due to the imbalance in the middle of negative and positive samples, the author experienced classification networks depend on the block. The classification network with the highest certainty was preferred and used as a backbone of the picture segmentation network—Mask R-CNN, which achieved excellently on ordinary pictures. Finally, Mask R-CNN design experienced on COCO knowledge set fine-tuned for sector pulmonary nodules. The designs were certified on the LIDC-IDRI dataset. A segmentation design that depends on the fast filling technique was proposed which divides the picture into a part with the same features, that were again merged by connecting parts developing with k-means. The proposed design was related to effective contour designs and two modernized deep learning systems [19]. It arrived with a good comprehensive efficiency than effective contour designs, having equal results for DBResNet but minor efficiency than 3D-UNet.

An existing method aims to provide a survey of potential and current approaches for AI schemes in pathology picture investigation, with intensity on lung cancer [20]. The author outlined the present opportunities and challenges in lung cancer cytology picture investigation, explained the latest deep learning improvements which probably impact digital cytology in lung tumor, and outlined the current approaches of deep learning designs in lung tumor prognosis and diagnosis. Another method in literature [21] employed an ML-CNN that investigated the issue of lung nodule malignancy classification. ML-CNN contains three CNNs to extract multi-scale appearances in lung nodule CT pictures. Moreover, the author smashes the output of the ending pooling layer toward a one-dimensional vector to each level and concatenates them. The strategy assisted in improving the conducting of the design. The ML-CNN was tested for ternary analysis of lung nodules (malignant, benign, and indeterminate lung nodules).

The examination with a deep learning design with a kNN classifier developed a success rate in determining lung cancer. The dataset used was a publicly reachable resource SPIE-AAPM. The author utilized data augmentation on the practice dataset for enlarging the dataset and CNN for exact similar features [22]. Extracted features against CNN utilized as input for kNN classifier along cross-validation. Other methods involve fusion-based methods where two modalities are fused in the frequency domain to

CORRECTED PROOF

detect the region of interest [23]. Histopathological image processing [24] also plays a key role in the detection of abnormalities in the cell count owing to the propagating cancer cells. Keras library and CNN model are utilised throughout the simulation model. Shiny web platform is used to create web applications. The results of the experiments revealed that the CNN architecture had high predictive performance indicators of benign or malignant lung disease on CT scans images [25]. To train features at multiple sizes, a multiscale CNN with a parallel type of configuration is used. The loss function is utilised in the network training process to mitigate the detrimental impact of class imbalance on heart disease outcomes [26].

3. Proposed work

3.1. Machine learning

Machine learning models have exceeded the state-of-the-art in several image identification tasks during the last few years. While convolutional neural networks (comp net) have been around for a long time, their performance has been restricted due to the size of the training sets and the scale of the networks under consideration. Comp-net is a type of AI that is so far been most popularly used for image analysis although image analysis has been the most widespread use of CNN classification problem. Disadvantages of ANN over CNN are primarily attributed to too much time consumption. U-net architecture is a classic for image segmentation. This model is advanced over conventional networks. Here, various convolution layers and pooling layers are used to achieve accuracy. U-nets are specially arranged where the first layer is just an input layer. This layer reflects the dimension or depth which typically means it is a color image. For example, 24×24 is considered as an input image for the first layer of CNN. Further, the second layer dimension and size of the image may alter depends on the weight.

The objective of this work is to effectively present a novel algorithm for segmentation and classification between cancerous and non-cancerous lung nodules. The initial step in the proposed technique is to extract many abnormal and normal samples from the digital camera. The sample is collected from a digital camera, and the characters are then collected in the database. To enhance image data, a pre-processing method is used which increases some figure features or defeat unwanted distortions for more processing. It

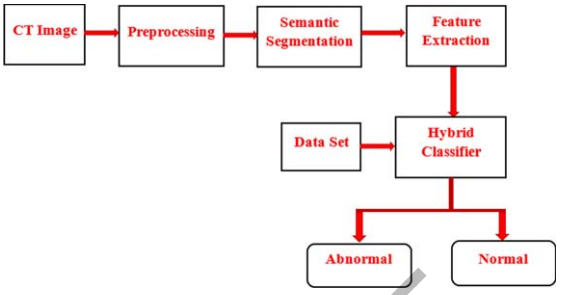


Fig. 2. Block diagram of the proposed method.

is essential for minimizing the development of distortion present in imaging devices like light fluctuation, to take out blueness and at a similar time pre-processing is needed for extracting unwanted regions from the figures and few times used for increasing the features of images such as boundaries, texture, and line of an image which easily split the content of figures into two parts, unwanted and wanted image contents. Figure 2 depicts the flow diagram of the proposed technique. Thus, lung region boundaries and backgrounds are eliminated in a pre-processing technique. Furthermore, to remove the noises such as salt-and-pepper and white noise that are familiar issues present in images, a median filtration is used for extracting the unwanted noise and thus by retrieving the image sharpness. Every pixel is displaced by the median value from the nearest pixels. A window size of 3 * 3 is utilized in the filter.

The adaptive median filter is one of the greatest filters between conventional filters that separate the speckle noise. The spatial processing for preserving the edge information and removing non-impulsive noise is made through an adaptable median filter which plays an important role. In adaptive median filter, the tiny structure in the edge and images are attained and the window dimensions changes according to every pixel. After the removal of noise through the adaptive median filter, the segmentation process is performed. This means to divide or segment an image into various parts since it adds more sense to the image and is easy to analyze and as well as make the simpler image.

3.2. U-net segmentation network

U-net architecture is designed for semantic segmentation of biomechanical images. Here, a 572×572 input image with 64 characteristics that may be modified with your own model has been

CORRECTED PROOF

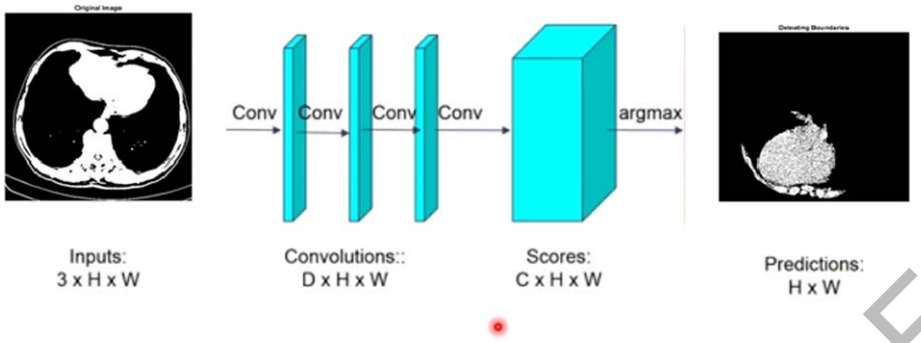


Fig. 3. Block diagram for abnormality detection using CNN.

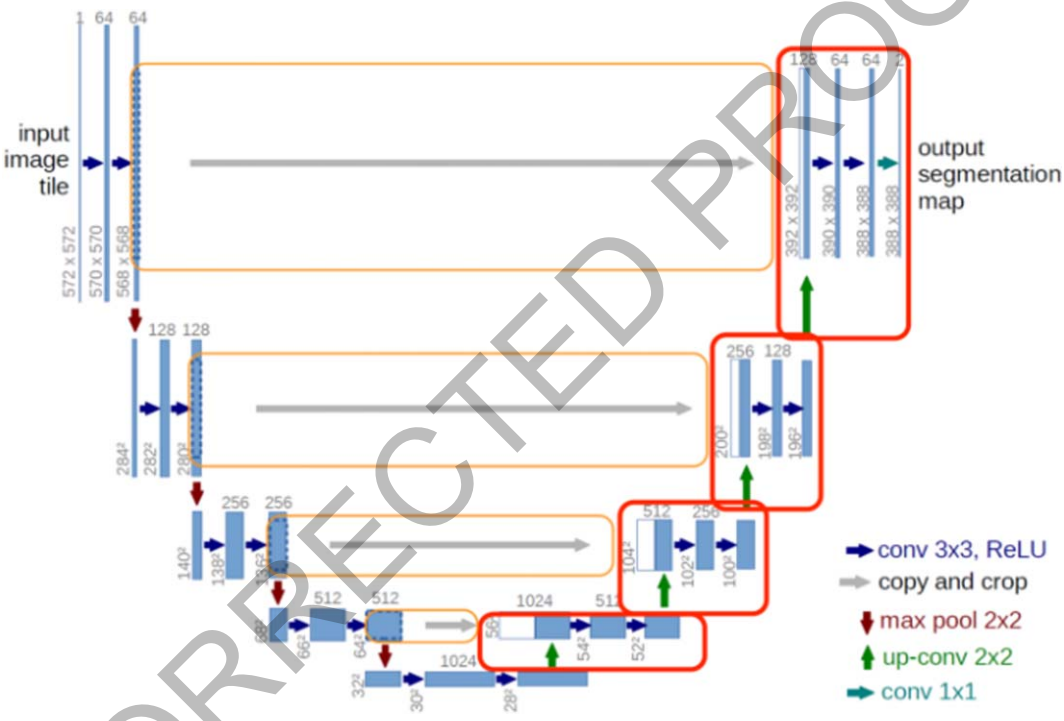


Fig. 4. Shows the U-net model for segmentation.

CORRECTED PROOF

created. Input image with three channels is used. Semantic segmentation is not just for recognition but also used for labeling. Generally, the Auto encoder architectures illustrate the left side as encoding and the right side as decoding network. Semantic segmentation for fully convoluted network input is 3xHxW, convoluted by D x H x W, scores are C x H x W finally predicted by HxW as shown in Fig. 3 for biomedical image segmentation most probably U-net architecture is used widely. So, this network is again very similar for auto encoder and decoder. This architecture includes Conv2D is convolution layer with padding and kernel, Maxpooling, cropping. Concatenate and Upsampling etc.

Figure 4 illustrated the U network architecture for detecting abnormality. The input image and segmentation maps are utilized to train the network using gradient descent. Because of the unpadded convolutions, the output is a constant border width that is smaller than the input. The cross-entropy is expressed as in (1).

$$E = \sum_{x \in \Omega} w(x) \log(p_{\ell(x)}(x)) \tag{1}$$

Whereas P(x) represents the possibility of activity x in P, Q(x) determines the degree of event W(x) and log represents the higher modulation logarithm, indicating that the values are in bits. If you use the base-e or overall level rather than, the output will be in nats.

A classification procedure was required to identify an object that was categorized. In this example, SVM is trained to conclude whether a feature taken from an image is a nodule. SVM, like other classification algorithms, has two stages: training and testing. Below equation 2 is used for computing the SVM classifier:

$$\left[\frac{1}{n}\sum_{i=1}^{n}\max\left(0,\ 1-y_i\left(\mathrm{w}^T\mathrm{x}_i-b\right)\right)\right]+\lambda\left\|\mathrm{w}\right\|^2. \tag{2}$$

Early detection of a nodule can improve a patient's chances of survival. Identifying the stages of cancer can also aid in the delivery of appropriate treatment to patients. The radiologist faces a difficult task in interpreting the diagnostic imaging because CT images have high dimensionality, and the nodule could be small. In these methods, a contemporary CNN architecture was suggested for identifying anomalies in the input picture. Using deep networks, this technique recognizes the lung nodule automatically. Image analysis has traditionally relied on a basic CNN architecture for detection and classification. Here a modern CNN architecture is used for diagnosis lung nodule detection. The system begins with a single Computer Tomography scan. It extracts one picture from the entire scan and divides it into 64 patches. These patches are numbered arranged in the order in which they appear in this picture. The classification component of the CNNs' design will 6 categorize as discussed above. Given that, lung nodule diameters generally range from 3 to 30 mm, the scale of these patches to 64×64 pixels to maintain all nodule feature information. This, however, might lead to a failure, including the misdiagnosis of small lumps. The Ist conv layer C1 is 33 in size with 32 kernels, while the IInd layer C2 is 33 in size with 64 kernels. And C2 has 2 strides. The strides are programmed to minimize the dimension of feature maps as well as the number of CNN weights. Every kernel generates a 2D picture. The important structure of the network, which is a residual block. It is made up of three distinct convolutional layers. A skipped link will be made between the input of the residual block and the end of the conv block. As a result, the ResNet may access previous activations that were not changed in the convolutional block. The Xavier approach initializes the kernel values, which may then be modified during CNN training through backpropagation. In the conv layer, utilized Leaky Recti linear Unit as the activation function. In contrast to standard activation functions like tanh and sigmoid, is relatively simple. When $x>0$, the activation f(x) is f(x) = x, and when x 0, it is f(x) = axe. Finally, the last layer of our network, instead of a completely linked layer, employed a GAP layer. First selected a 4×4 kernel size, which means that each feature map would be followed by a single output. When compared to a completely linked layer, it can minimize a huge number of parameters. In addition, we employed the batch normalization layer to control over fitting and accelerate network convergence.

The performance has been evaluated with better outcomes. Accuracy is mentioned as an absolute rate of classification that equals the overall addition of exact organization over the overall addition of correct and incorrect organization multiplied by 100. The specificity is mentioned for the entire division of true positive in the case of the entire of true positive and false negative when sensitivity is mentioned as true negative in the case of false positive and true negative. True positive (T_a) presents when correct organization to the right picture is made i.e. when a common brain is differentiated as common when false-negative (F_b) presents when a common brain is incorrectly proceeding as diseased. True negative (T_b) presents when correct organization to the right picture is made i.e. when an affected picture is classified as being affected when false positive (F_a) presents while an affected picture is incorrectly differentiated to be normal.

$$Specificity = \frac{T_a}{T_a + F_b} * 100,$$
$$Sensitivity = \frac{T_b}{T_b + F_a} * 100 \tag{3}$$

$$Accuracy = \frac{T_b + T_a}{T_a + T_b + F_b + F_a} * 100 \tag{4}$$

Where in Equations (3) and (4), T_a is true positive, F_b is a false negative, T_b is a true negative and F_a is false positive, and from this above equation, depicts high accuracy in the proposed technique. The pseudo-code for the proposed model is condensed as follows.

CORRECTED PROOF

Pseudocode:

Input: Dataset of CT lung image
Output: Segmented and Classifications of abnormality
Initialize paramaters w,h,x,a,b

Initialize work CNN and SVM classifiers
For filtering techniques
edgerow : = (width/2)
edgecolumn : = (height/2)
Create a U-Net depth of 3
Train U net with 1000 iterations
Let f id the features
Define no. of feature and SVM
If (y(w, $x = b$) $= 0$;
Else if(y(w,x + b)–1 < 0;
for each epoch
For all training set:
Create the U-Net network
$dj\ (k) = P\ (S1 = Ek|C1 = hj)$
Streamed data (read)
Conversion (float data)
Array format (Store)
End
Array(feature) = array_[SVM*array[SVM*Feature]
Distance_value = array_test [feature]
$dj\ (k) = P\ (S1 = Ek|C1 = hj)$
Return 1
Classify data using SVM and CNN
$w\ (\alpha) = \sum \alpha i \alpha j y i y j m i = 1\ K\ (xi, xj).$
Load training images and pixel labels into the workspace.
$L(t) = {}^{1}/_{2} \sum (\text{train}_{p(n)} - \text{train y(n) 2}$
Prdict
train_p (predict) is calculated.
Loss (t) is recalculation
end
end

4. Results and discussion

The outcome of the recommended scheme is achieved by using MATLAB software. Initially, median filtration is implemented. Later, classification is done on pictures in GUI by utilizing CNN and SVM classifier, in MATLAB that shows the abnormality or normality of lung. The scheme user interfaces were created and implemented on MATLAB 7.10a running on 4GB RAM. The lung CT scans utilized in our experiment were obtained from the Lung Image Dataset Consortium collection. Currently comprises 1000 cases with 30,000 above Ct scan images with 512×512 pixel size are available in the database. The outcomes are shown for clarity and more studies. A sample set of images taken as input for the proposed work is shown in Fig. 5.

The noise models used are pepper and salt noise and speckle noise which are more prevalent in medical image processing. The enhanced images are depicted in Fig. 5. During the pre-processing stages, the boundaries are removed as shown in Fig. 6.

In the segmentation step, the pre-processed picture is divided into certain portions, and extracts the cancer region against the scanned CT picture becomes the sole objective. A combination of supervised and unsupervised learning is used in the proposed work through CNN and SVM models.

The pictures collected were moved into a neural network for training and resting pictures used for validation and testing. These pictures are early treated, pre-processed, and then segmented before being moved to a neural system. The CNN extracts attributes like roughness and texture from pictures and executes exact classification sequences, in sync with train sets. The CNN classifies with a specified number of neurons it is trained with. CNN and SVM classifiers are used to resolve whether the CT scan pictures are benign or malignant. Figure 7 depicts a segmented image.

The recommended methodology displays good performance compared to the existing conventional models. The methodologies await different features still missing the key feature e.g., nodules size to find lung lumps at an initial phase and more to allocate them toward benign and malignant lumps. The nodules size measurement is used that is the main factor to radiologists for analyzing the benign and malignant nodules.

The total training time taken by classifiers to observe, study, and learn the picture confer to given design features and structures. Every classifier investigates the picture in its capability and the time for this training is checked on. Recognition of pictures appears when a classifier is ready to accurately detect and advise itself with what has been experienced. Recognition time plays a key role in the classification of medical pictures, as longer detection time leads to higher memory consumption that affects corresponding. Thus the CNN and SVM pose a shorter time as opposing to the other models. Table 1 displays the comparative survey of the classification accuracy and segmentation time. The CNN and SVM ready to give an exact classification of outcomes.

The major contribution of this study is to offer a learning technique for lung disease based on CNN with classifiers like SVM, MLP and LSTM that can categories the activities. The classifier is made up of a CNN and SVM algorithm that is combined.

In this techniques also integrated the same pretained U net model that was used to extract features

CORRECTED PROOF



Fig. 5. Samples Lung CT images taken for experimentation.

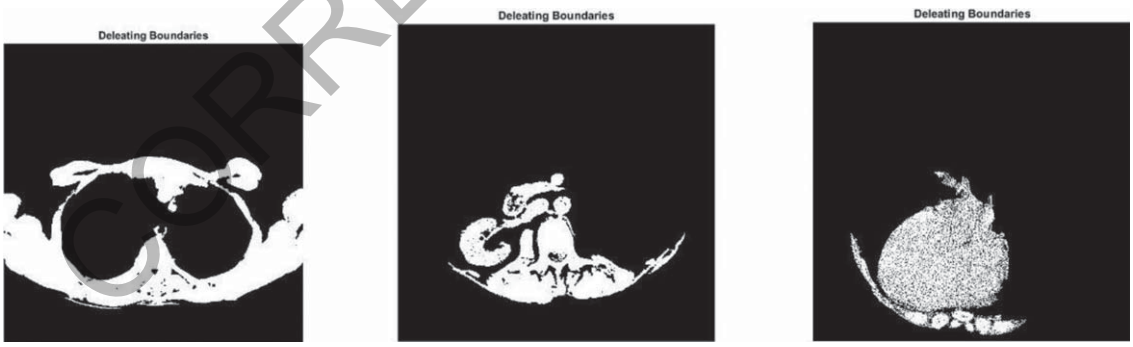


Fig. 6. Boundary eliminated lung images.

with a MLP classifier and LSTM. The findings demonstrate that employing a SVM classifier produces the best results.

To address the present difficulties, we created three strategies based on feature-based methods and deep learning approaches such as SVM, MLP, and LSTM. DL approaches are learned on source data without even any feature extraction, while functionality classifier is trained on manually derived features. It is expected that this will be the sole use of automatic feature engineering that focused on Deep learning.

It could be observed from above Table 1 that the present hybrid model's classification achieved 97% accuracy that is very higher than the other exist-

CORRECTED PROOF

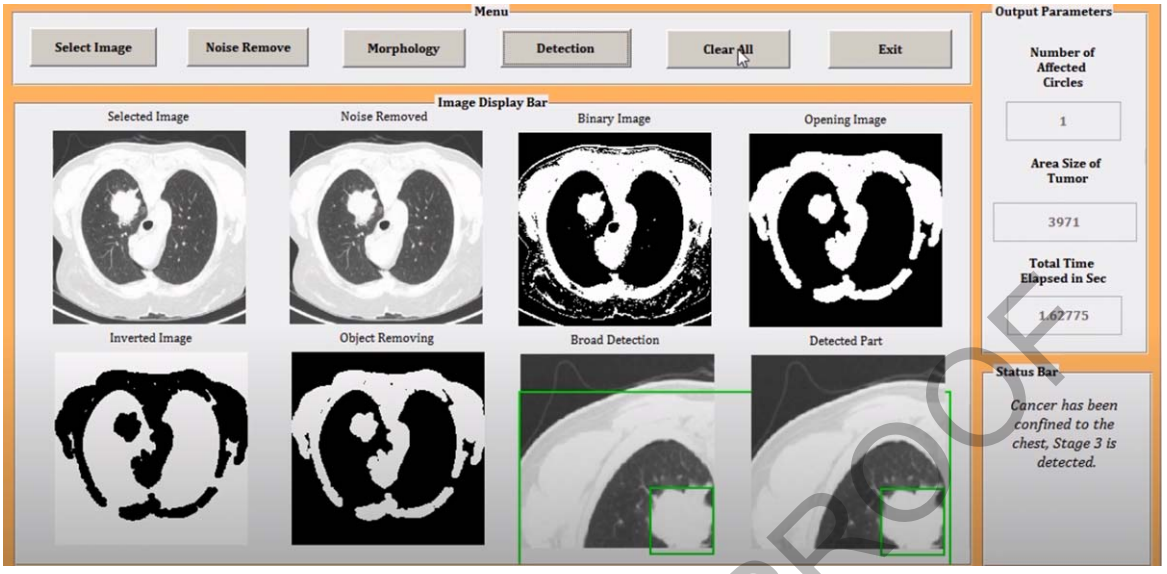


Fig. 7. GUI Segmented results of abnormality.

Table 1
Comparative survey of computation time to segmentation & Classification accuracy

Technique	Computation time (s)	Classification Accuracy (%)
Proposed Hybrid model [CNN + SVM]	**0.26 s**	**97**
CNN + LSTM	0.46 s	96.67
CNN + MLP	0.28 s	95

ing methods. The observations of specificity, recall, and precision is compared and presented below. Classification accuracy is yet another crucial metric that reflects the detection of cancerous from non-cancerous images. It is depicted in Fig. 8 and tested against an increasing number of sample images.

The sensitivity analysis is projected in Table 2, the high sensitivity values are proposed through HLM

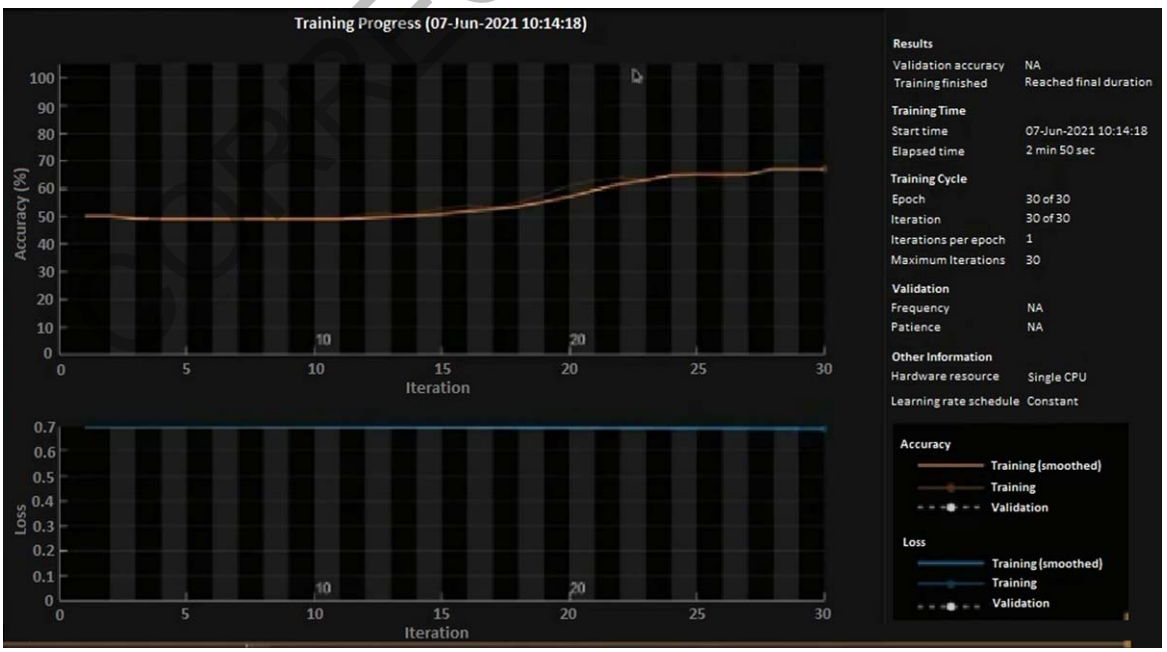


Fig. 8. Overall Classification accuracy.

CORRECTED PROOF

Table 2
Sensitivity analysis for detection of lung nodules

Sample No.	Techniques		
	CNN + MLP	CNN + LSTM	HLM (CNN + SVM)
1	0.6314	0.6498	0.7024
2	0.6206	0.6365	0.7055
3	0.6444	0.7210	0.7180
4	0.7192	0.7295	0.7259
5	0.6578	0.7109	0.8310
6	0.7154	0.7099	0.7877
7	0.7024	0.7045	0.7018
8	0.5399	0.6543	0.6894
9	0.6234	0.6650	0.7007
10	0.6111	0.6198	0.6898

reflect a high degree of classification and segregation between cancerous, non-cancerous lung nodules described in this section.

5. Conclusion

Lung cancer is one of the most dangerous ailments worldwide. In the course of disclosing lung cancer, this work plays a significant role in evading grave phases and decreasing its growth in the world. The efforts for diagnosing lung cancer through image processing models have been done. First, the CT scan was taken, and the images were obtained, the captured images were processed, and the tumor or cancer region was diagnosed and detected. In the pre-processing stage, the adaptive median filter technique was used to filter the image distortion. They aid in identifying various mark boundaries and dimensions of cancerous cells. Then, classifiers were implemented. In the classification section, CNN and SVM classifiers were used. CNN and SVM techniques in a diagnostic system helped in attaining high accuracy level. This classification depicts which lung figure seems to be abnormal and normal in early diagnoses. Lung cancer disease prediction assists doctors in devising better treatment plans and providing victims with prompt diagnoses. However, the contrast between CT scan images should be done for a better outcome, for prior lung cancer diagnosis.

References

[1] M. Bari, A. Ahmed, M. Sabir and S. Naveed, Lung cancer detection using digital image processing techniques: A review, *Mehran University Research Journal of Engineering & Technology* **38** (2019), 351–360.

[2] H. Cao, H. Liu, E. Song, C. Hung, G. Ma, X. Xu, R. Jin and J. Lu, Dual-branch residual network for lung nodule segmentation, *Applied Soft Computing* **86** (2020), 105934.

[3] H. Cao, H. Liu, E. Song, G. Ma, X. Xu, R. Jin, T. Liu and C.C. Hung, Two-stage convolutional neural network architecture for lung nodule detection, *arXiv preprint arXiv:1905.03445* (2019).

[4] M.P. Chander, M.V. Rao and T.V. Rajinikanth, Detection of lung cancer using digital image processing techniques: a comparative study, *International Journal of Medical Imaging* **5** (2017), 59–62.

[5] X. Dong, S. Xu, Y. Liu, A. Wang, M.I. Saripan, L. Li, X. Zhang and L. Lu, Multi-view secondary input collaborative deep learning for lung nodule 3D segmentation, *Cancer Imaging* **20** (2020), 1–13.

[6] P. Joon, S.B. Bajaj and A. Jatain, Segmentation and detection of lung cancer using image processing and clustering techniques, In *Progress in advanced computing and intelligent engineering*, Springer, Singapore, (2019), 13–23.

[7] S.K. Lakshmanaprabu, S.N. Mohanty, K. Shankar, N. Arunkumar and G. Ramirez, Optimal deep learning model for classification of lung cancer on CT images, *Future Generation Computer Systems* **92** (2019), 374–382.

[8] T. Meraj, A. Hassan, S. Zahoor, H.T. Rauf, M. Lali, L. Ali and S.A.C. Bukhari, Lung nodules detection using semantic segmentation and classification with optimal features, *Neural Computing and Applications*, 201909.0139 (2019), 1–14.

[9] C.M. Nam, J. Kim and K.J. Lee J, Lung nodule segmentation with convolutional neural network trained by simple diameter information, 1st Conference on Medical Imaging with Deep Learning (MIDL 2018), Amsterdam, The Netherlands. (2018).

[10] N. Nasrullah, J. Sang, M.S. Alam, M. Mateen, B. Cai and H. Hu, Automated lung nodule detection and classification using deep learning combined with multiple strategies, *Sensor* **19** (2019), 3722.

[11] M. Rahman, A Deep Learning Approach to Detect Lung Cancer Using Alexnet and kNN (Doctoral dissertation, Daffodil International University) (2021).

[12] B.K. Samhitha, S.C. Mana, J. Jose, R. Vignesh and D. Deepa, Prediction of Lung Cancer Using Convolutional Neural Network (CNN), *International Journal* **9** (2020).

[13] M. Savic, Y. Ma, G. Ramponi, W. Du and Y. Peng, Lung Nodule Segmentation with a Region-Based Fast Marching Method, *Sensors* **21** (2021), 1908.

[14] J. Samuel Manoharan, Improved Version of Graph-cut Algorithm for CT images of Lung Cancer with Clinical Property Condition, *Journal of Artificial Intelligence* **2** (2020), 201–206.

[15] J. Samuel Manoharan and A. Sathesh, Early diagnosis of lung cancer with probability of malignancy calculation and automatic segmentation of Lung CT scan images, *Journal of Innovative Image Processing* **2** (2020), 175–186.

[16] K. Senthil Kumar, K. Venkatalakshmi and K. Karthikeyan, Lung cancer detection using image segmentation by means of various evolutionary algorithms, *Computational and Mathematical Methods in Medicine*, doi.org/10.1155/2019/49098462019.

[17] A.K. Tiwari, Prediction of lung cancer using image processing techniques: a review, *Advanced Computational Intelligence: An International Journal* **3** (2016), 1–9.

[18] S. Wang, A. Chen, L. Yang, L. Cai, Y. Xie, J. Fujimoto, A. Gazdar and G. Xiao, Comprehensive analysis of lung cancer pathology images to discover tumor shape and boundary

CORRECTED PROOF

features that predict survival outcome, *Scientific Reports* **8** (2018), 1–9.

[19] S. Wang, D.M. Yang, R. Rong, X. Zhan, J. Fujimoto, H. Liu, J. Minna I.I. Wistuba, Y. Xie and G. Xiao, Artificial intelligence in lung cancer pathology image analysis, *Cancers* **11** (2019), 1673.

[20] Z. Wu, Q. Zhou and F. Wang, Coarse-to-Fine Lung Nodule Segmentation in CT Images with Image Enhancement and Dual-Branch Network, *IEEE Access* **9** (2021), 7255–7262.

[21] J. Xiong, X. Li, L. Lu, L.H. Schwartz, X. Fu, J. Zhao and B. Zhao, Implementation strategy of a CNN model affects the performance of CT assessment of EGFR mutation status in lung cancer patients, *IEEE Access* **7** (2019), 64583–64591.

[22] D. Yasmeen, S.S. Nisha and M.M. Sathik, Analytical Study of Various Filters in Lung CT Images, *International Research Journal of Engineering and Technology* **6** (2019), 322–325.

[23] N. Kathiresan and J.S. Manoharan, A Comparative Analysis of Fusion Techniques Based on Multi Resolution Transforms, *National Academy of Science Letters* **38** (2015), 61–65.

[24] J.S. Manoharan, V. Parthasaradi and K. Suganya, A Spatio-Frequency Domain Anisotropic Filtering for Contrast Enhancement of Histopathological Images, *Annals of the Romanian Society for Cell Biology* (2021), 4945–4958. Retrieved from https://www.annalsofrscb.ro/index.php/journal/article/view/5982.

[25] A.K. Arslan, An Intelligent System for the Classification of Lung Cancer Based on Deep Learning Strategy, *2019 International Artificial Intelligence and Data Processing Symposium (IDAP)*, (2019), 21–22. 10.1109/IDAP.2019.8875896

[26] X. Li, A Combined Loss-Based Multiscale Fully Convolutional Network for High-Resolution Remote Sensing Image Change Detection, *IEEE Geoscience and Remote Sensing Letters* 2021. 1–5, 10.1109/LGRS.2021.3098774.

CORRECTED PROOF